Journal of Molecular Liquids 221 (2016) 1029–1033

Contents lists available at ScienceDirect

Journal of Molecular Liquids

journal homepage: www.elsevier.com/locate/molliq

Conducting PANI stimulated ZnO system for visible light photocatalytic degradation of coloured dyes

R. Saravanan [a,b,*], Elisban Sacari [b], F. Gracia [a,*], Mohammad Mansoob Khan [c], E. Mosquera [b], Vinod Kumar Gupta [d,e]

[a] Department of Chemical Engineering and Biotechnology, University of Chile, Beauchef 850, Santiago, Chile
[b] Nanoscale Materials Laboratory, Department of Materials Science, University of Chile, Avenida Tupper 2069, Santiago, Chile
[c] Chemical Sciences, Faculty of Science, Universiti Brunei Darussalam, Jalan Tungku Link, Gadong BE 1410, Brunei Darussalam
[d] Department of Chemistry, Indian Institute of Technology Roorkee, Roorkee 247 667, India
[e] Department of Applied Chemistry, University of Johannesburg, Johannesburg, South Africa

ARTICLE INFO

Article history:
Received 6 May 2016
Received in revised form 11 June 2016
Accepted 15 June 2016
Available online 23 June 2016

Keywords:
Zinc oxide
PANI
Nanocomposite
Visible light
Methyl orange
Methylene blue

ABSTRACT

In this report, the polyaniline (PANI)/ZnO nanocomposite system exhibits superior degradation of methyl orange and methylene blue under visible light condition, due to the intermolecular interaction between conducting PANI sponsoring more number of electrons to the conduction band of ZnO nanoparticles. The pure ZnO and the different mole ratios of PANI into ZnO catalysts were prepared by precipitation followed by sonication process. The bandgap of the nanocomposite system revealed in the red region was estimated by Tauc plot. The X-ray diffraction results indicate that the high quantity of PANI into ZnO system reduces the crystallite size and also the crystallinity of the materials. On comparing with the other prepared materials, PZ1.5 illustrated higher degradation of methyl orange and methylene blue. The reason for high catalytic activity and their mechanism of visible light activities were discussed in this paper.

1. Introduction

At present, the investigators are focusing numerous studies on nano semiconductor catalysts due to its exciting properties in several applications [1–4]. Goesmann et al. has explained that the nano materials express smaller size, larger surface area and fascinating quantum dependent properties which are entirely different from bulk materials. Therefore, the nanomaterials exhibit unbelievable efficiency for different applications [5]. Between other semiconductors, the large energy gap semiconductors like titanium oxide (TiO_2), cerium oxide (CeO_2) and zinc oxide (ZnO) show excellent results for various applications like sunscreen, paints, solar cells, antibacterial activity, photocatalyst, biosensor, gas sensor and so on [6–8]. For commercial consideration, ZnO is superior than other two semiconductors since it is too inexpensive. However, ZnO is restricted in degrading contaminants under visible light due to insufficient energy of their large band gap [9–13].

Nowadays, the ecosphere is facing a challengeable assignment for inefficient energy and environmental pollutions [14–15]. This is very significant and hot topic for the researchers in these days. Different kinds of polluting proxies present in the surrounding due to huge population leads numeral industrial unit, vehicles and so on. In some circumstances, untreated harmful chemical waste water directly spoils the fresh water sources that extent variety of health dangers to human life [14–16]. In the current development, the investigators utilize the metal oxide nanoparticles for waste water treatment by several chemical and bio techniques [16]. The photocatalytic approach is the best opted way to decrease the impurities present in the water under various wavelengths of light irradiation [17–19]. This process is a unique way of handling waste products, since it needs smaller amount of catalysts and generates almost zero or very less harmful by-products [17–19].

Generally, the ZnO based hybrid nanocomposite materials such as ZnO/metal, ZnO/metal oxide and ZnO/polymer show visible light photocatalysis, because of the intermediate states present in the nanocomposite which absorbs visible light that prompts electrons and holes during the photo reaction [9–13,20,21]. Recently, we reported that ZnO combined with CdO, CuO, CeO_2 and Mn_2O_3 can effectively prevents electron-hole recombination and this allows extending the degradation of pollutants from UV to visible light, because of its synergetic

* Corresponding authors at: Department of Chemical Engineering and Biotechnology, Faculty of Mathematics and Physical Sciences, University of Chile, Beauchef 850, Santiago, Chile.
E-mail addresses: saravanan3.raj@gmail.com (R. Saravanan), fgracia@ing.uchile.cl (F. Gracia).

http://dx.doi.org/10.1016/j.molliq.2016.06.074
0167-7322/

effect between the two semiconductors [10–12,22]. On the other hand, the surface defect induced ZnO/Ag (metal) system inhibits electron-hole pairs during the photocatalytic process, which led to improve the efficiency of MB degradation in 2 h under visible light [9]. Further, polyaniline (PANI) is one of the best conductive polymers due to –NH- groups present in the chain. The PANI holding wide-ranging of applications like supercapacitors, sensors, batteries and organic coating prevent the corrosion and so on, since it has high stability and conductivity [23–26].

The objective of the present work is to reduce the band gap of ZnO by adding different mole ratios (1 M, 1.5 M and 2 M) of PANI and was synthesized by simple precipitation followed by sonication. The change of structural and morphological observation of pure ZnO and modification of PANI/ZnO were investigated with the use of XRD and TEM results. The optical bandgap of the materials were determined by Tauc plot based on UV–Vis absorption results. The prepared catalysts were examined to degrade methyl orange (MO) and methylene blue (MB) dyes. Moreover, the photocatalytic results and their mechanism are discussed in detail.

2. Experimental

2.1. Materials

The photocatalytic degradation of methyl orange (MO) and methylene blue (MB) dyes for the synthesis of pure ZnO and polyaniline (PANI), the required chemicals zinc acetate dihydrate ($Zn(CH_3COO)_2 \cdot 2H_2O$), diethylene glycol, ammonium peroxydisulphate (APS) and sodium hydroxide (NaOH) were purchased from Sigma-Aldrich. These chemicals were used without any further purification. All the aqueous solutions were prepared using double distilled water.

2.2. Pure nano ZnO preparation

The nano ZnO was prepared by several procedures [27]. When compared with the other methods, precipitation method is simple, inexpensive and the duration of synthesis is less and cost effective [27]. Primarily, 0.1 mol of zinc acetate dihydrate was dissolved in 500 ml of double distilled water under vigorous stirrer at 600 rpm. Then 0.05 mol of sodium hydroxide was added slowly into the initial solution. Simultaneously, the pH of the solution was maintained between 7 and 8. The persistence of the above step explained that when $Zn(CH_3COO)_2 \cdot 2H_2O$ reacts with NaOH, precipitate of zinc hydroxide was obtained. Then the precipitation powder was washed several times, filtered, and then dried at room temperature. The collected powder was calcined at 400 °C for 1 h due to the removal of hydroxide and the formation of zinc oxide.

2.3. PANI/ZnO nanocomposites preparation

For the preparation of nanocomposite, 0.5 M of diethylene glycol solution was mixed with 1.0 g of ZnO nanoparticles (prepared by the above procedure) and the solution was sonicated (~42 kHz). Then different mole ratios of (1 M, 1.5 M and 2 M) polyaniline were mixed with 0.2 M of ammonium peroxydisulphate (APS) under vigorous stirrer at 600 rpm for 2 h. This polymerization solution was added drop wise into the diethylene glycol/ZnO solution. The resulting mixture was sonicated overnight. Finally, the sample was recovered and followed by filtering, washing, and finally drying at 50 °C for 10 h under vacuum condition. The synthesized samples were labeled for easy identification as PZ1, PZ1.5 and PZ2 respectively.

2.4. Photocatalytic activity

The prepared pure ZnO and the different mole ratios of PANI/ZnO nanocomposites system were used in degrading MO and MB solution under visible light condition. The procedure of the photoreaction was described in our previous reports [9–13,28,29]. The whole photocatalytic reaction was maintained at a constant temperature of 25 °C with a projection lamp (7748XHP 250 W, Philips) fitted in the photo reactor for the source of visible light irradiation. Primarily, 100 mg of the synthesized catalyst was mixed with 100 ml of dye solutions (initial concentration) in a 500 ml cylindrical beaker covered by circulating $K_2Cr_2O_7$ solution to avoid exposing UV radiation. Under dark condition, the mixture of reaction suspension was vigorously stirred for 30 min to establish adsorption/desorption equilibrium condition. The solution mixture was irradiated at uniform time interval. The irradiated solution was collected, then the catalysts were separated by centrifugation and filtration. Finally, the absorption spectra of initial and uniform time interval of the irradiated solution were found out by UV–vis absorbance spectroscopy.

$$\eta = \left[1 - \frac{C}{C_0}\right] \times 100 \quad (1)$$

where, η is the degradation efficiency, C_0 and C are the concentrations of the dye solution before illumination ($t = 0$) and after illumination of light for 't' minutes, respectively.

2.5. Characterization details

The crystal structure and crystallite size of the synthesized materials at room temperature was determined by X-ray diffraction using a D5000 diffractometer (Siemens, USA) with $CuK_{\alpha 1}$ ($\lambda = 1.5406$ Å) radiation. The morphology and size of the synthesized materials were confirmed by transmission electron microscopy (TEM, Tecnai G^2 20 S-TWIN, FEI Netherlands). The specific surface area of the catalysts was calculated using Brunauer–Emmett–Teller (BET, Micromeritics ASAP 2020, USA) equation. The band gap (Tauc plot) and the photocatalytic activity were measured by using a UV–Visible spectrophotometer (Perkin Elmer Lambda 35, USA).

3. Results and discussion

In this work, the properties of synthesized pure ZnO and the different mole ratios of PANI/ZnO photocatalytic materials were optimized by different techniques. Finally, the photocatalytic ability of the materials was found by the degradation of MO and MB solution under visible light irradiation.

The crystallite size and structure of the prepared materials were analyzed by XRD. Fig. 1(a) illustrates the pure ZnO material shows very sharp peaks compared with PANI/ZnO (Fig. 1 b to d) nanocomposite system. All the hkl planes and 2Θ values are agreed with the JCPDS

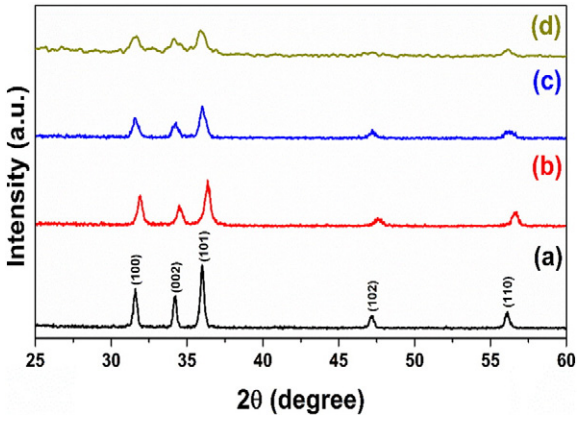

Fig. 1. XRD patterns of (a) ZnO, (b) PZ1, (c) PZ1.5 and (d) PZ2.

Table 1
Crystallite size, BET surface area, TEM particle size and band gap of the synthesized pure ZnO and different ratio of PANI/ZnO photocatalysts.

Samples	Crystallite size D (nm)	BET surface area (m^2/g)	TEM PARTICLE SIZE (NM)	Band gap based on Tauc polt (eV)
Pure ZnO	24.6	43.3	28	3.21
PZ1	20.3	44.2	25	2.99
PZ1.5	14.6	46.5	15	2.67
PZ2	9.8	47.8	Agglomeration	2.59

card number 79-0205. Scherrer formula was used to determine the crystallite size (D) of the synthesized catalyst [30].

$$D = k\lambda/\beta\cos\theta \quad (2)$$

where k is the shape factor (0.89), λ is the wavelength of X-ray (1.5406 Å), β is the line broadening at full width at half maximum (FWHM) in radians, and θ is the Bragg's angle.

Table 1 shows the values of the crystallite size of the synthesized photocatalysts. The PANI/ZnO nanocomposites revealed broad and low intensity peaks that signifies the indication of smaller size and possess low crystallinity nanocomposites. The declaration was promised with the previous reports [21,25–27,31–33]. The nanocomposite materials express low crystallinity and small size because of the intermolecular interaction between conducting PANI and ZnO nanoparticles [21,25,26]. From the XRD results, the nanocomposite materials exhibit smaller size that promotes high surface area which was confirmed by BET analysis and the results of BET specific surface areas are also tabulated in Table 1. The specific surface area of PANI/ZnO nanocomposites has increased because of the synergistic effect between PANI and ZnO nanoparticles which lead to the small size of nanocomposites [21,25,26].

The shape and size of the prepared catalysts were scrutinized by TEM images. Fine spherical shaped ZnO nanopartilces are obtainable in Fig. 2(a). The nanocomposites system clearly specifies that the ZnO nanoparticles are embedded in the PANI matrix, which was evidently shown in Fig. 2(b) to (d). When increasing the PANI quantity into ZnO nanoparticles, it gets dispersed and gives more aggregation, because of the intermolecular interaction between PANI and ZnO nanoparticles [21,25,26,31–33] which were evidently shown in Fig. 2 (d). This statement coincides with the previous literatures [21,25,26,33]. The particle sizes of the synthesized materials were determined and the values are presented in Table 1.

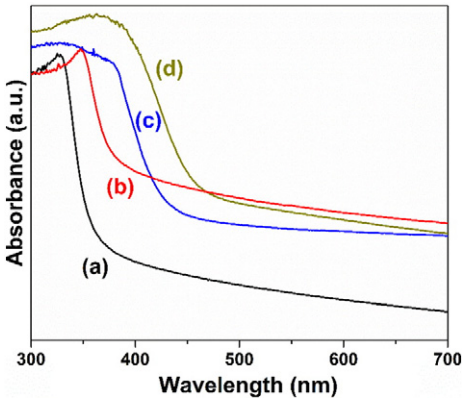

Fig. 3. UV–vis absorption spectrum of (a) ZnO, (b) PZ1, (c) PZ1.5 and (d) PZ2.

The band gap property of the synthesized catalysts was evaluated using Tauc plot established on UV–vis absorption spectra and their corresponding plots are shown in Fig. 3. From Fig. 3, it seems that the absorption edge of the nanocomposites is in the red region, which means higher wavelength that represents visible region than that of pure ZnO nanoparticles that shows lower wavelength. The band gap values were calculated using Tauc plot and the values are tabulated in

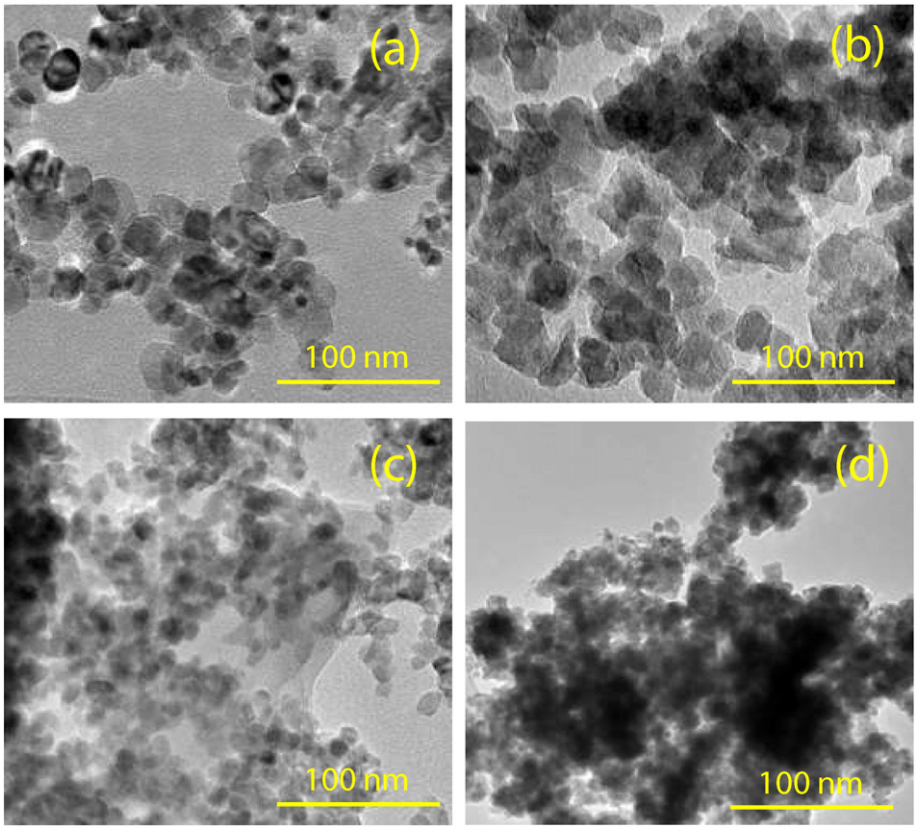

Fig. 2. TEM images of (a) ZnO, (b) PZ1, (c) PZ1.5 and (d) PZ2.

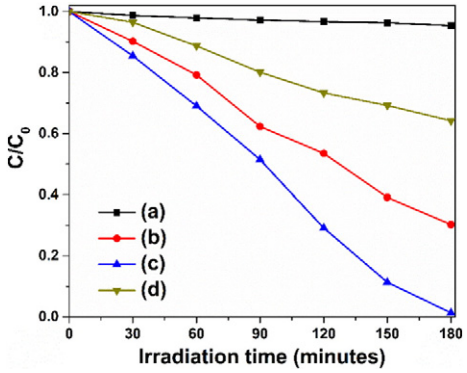

Fig. 4. Time course degradation curves for MO using (a) ZnO, (b) PZ1, (c) PZ1.5 and (d) PZ2 catalyst under visible light.

Table 1. The band gap value of the PZ2 nanocomposite is small when compared with other PZ1, PZ1.5 and ZnO catalysts. This result was in agreement with the previous reports [21,25,26]. Hence, the UV–vis absorption result evidently signified that the synthesized nanocomposite absorption is in the visible region of the electromagnetic spectrum. Therefore, we have concluded that because of the strong absorption in the visible region, it is predictable that the prepared nanocomposite systems might be photocatalytically active under visible light irradiation.

3.1. Degradation of MO and MB under visible light

The core part of this work is the photocatalytic degradation process that implicates under visible light irradiation using the prepared nanocomposite systems. The synthesized samples are employed for the degradation of MO and MB solution and their corresponding time dependent degradation curves which are represented in the Figs. 4 and 5.

The photocatalytic degradation efficiency of synthesized catalysts was determined by using Eq. (1) and their resultant percentage are listed in Table 2. The first order rate constants (k) of the photocatalytic reactions were calculated from the following equation:

$$k = \ln(C/C_0)/t \quad (3)$$

where C_0 and C are the concentrations of model dyes at the irradiation time 0 and t min.

The first order rate constant (k) value of the prepared samples (Table 2) evidently exposed that MB has degraded much more rapidly than that of MO degradation due to its simple structure [13]. On relating the result of degradation rate in both cases, PZ1.5 shows good efficiency under visible light.

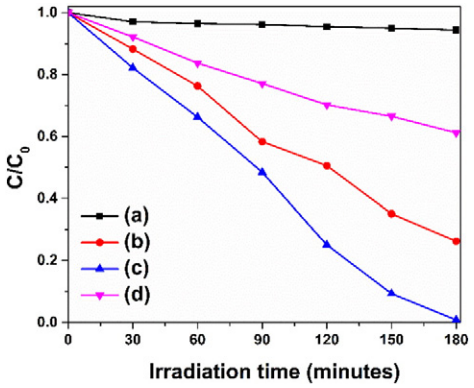

Fig. 5. Time course degradation curves for MB using (a) ZnO, (b) PZ1, (c) PZ1.5 and (d) PZ2 catalyst under visible light.

Table 2
MO and MB degradation efficiency and first order rate constant (k) values of all the prepared samples.

Samples	MO degradation rate (%) in 180 min	First order rate constant k (MB) 10^{-2} min^{-1}	MB degradation rate (%)in 180 min	First order rate constant k (MB) 10^{-2} min^{-1}
Pure ZnO	4.6	0.013	6.6	0.015
PZ1	69.8	0.607	74.6	0.674
PZ1.5	98.3	2.325	99.2	2.575
PZ2	24.7	0.226	39.7	0.227

Additionally, recycling process permits in finding out the stability and reusability of the nanocomposite materials. Fig. 6 shows the recycling ability of PZ1.5 nanocomposite. After undergoing recycling process of MO for three times under visible light irradiation, very slight variation was found. Thus, it was concluded that the nanocomposite exhibits good stability and reusability for the photocatalytic degradation of MO dye under visible light irradiation.

The PZ1.5 nanocomposite system displays superior degradation efficiency due to better crystallinity when compared with PZ2. In the meantime, the higher percentage PANI shows aggregation of particle which is another essential factor to reduce the degradation efficiency for PZ2 [27,34]. The illustration of schematic diagram (Fig. 7) symbolized the photocatalytic mechanism of the PANI/ZnO system.

When the photo (light) falls on the nanocomposite catalytic surface, the intermolecular interaction between conducting polymer PANI and ZnO occurs. The presenting PANI is excited in this system for $\pi \rightarrow \pi^*$ transition and produced electrons [21,25,26,35]. The excited electrons are transferred to the conduction band of ZnO which stimulates oxygen to give superoxide radical ion $O_2^{\bullet -}$ and consequently, the hydroxyl radical OH•. These radicals are more responsible for the degradation of MO [21,25,26,35]. For this reason, these nanocomposite systems exhibit photocatalytic activity of MO under visible light compared to pure metal oxides nanoparticles system. Hence, we finally conclude that the nanocomposite PZ1.5 material shows superior activity, because of its crystallinity and intermolecular interaction between conducting PANI and ZnO nanoparticles.

4. Conclusion

In this work, we effectively synthesized PANI/ZnO and pure ZnO by precipitation followed by sonication. The bandgap of the nanocomposite materials was displayed in the visible region which was established by UV–vis absorption spectroscopy. The nanocomposite PZ1.5 material shows superior activity because of its crystallinity, less aggregation of particles and intermolecular interaction between conducting PANI and ZnO nanoparticles. These are confirmed through TEM, XRD and BET techniques. The stability and reusability of the photocatalysts were

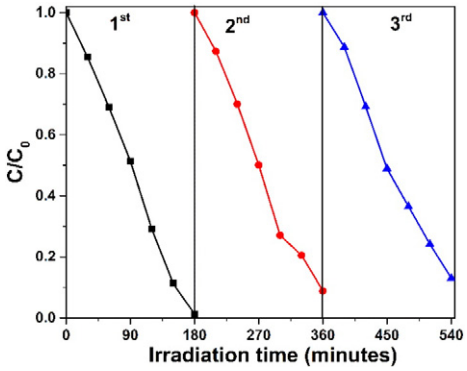

Fig. 6. Recycling ability of PZ1.5 nanocomposite for degrading MO under Visible light irradiation.

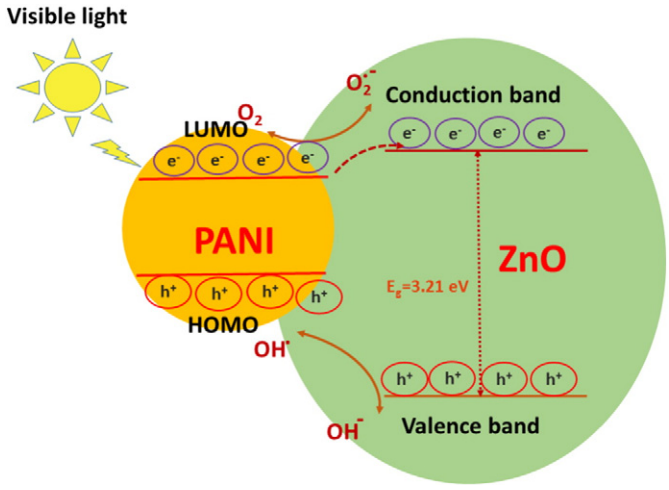

Fig. 7. Photocatalytic mechanism of PANI/ZnO system.

also found quite high. These results suggest that in future PANI/ZnO nanocomposite could be used for environmental remediation.

Acknowledgement

The authors (R.S and F.G) gratefully acknowledge the FONDECYT Post-doctoral Project No.: 3150631, Government of Chile, Santiago, for the financial assistance.

References

[1] J.A. Rogers, M.G. Lagally, R.G. Nuzzo, Synthesis, assembly and applications of semiconductor nanomembranes, Nature 477 (2011) 45–53.
[2] G. Jia, et al., Couples of colloidal semiconductor nanorods formed by self-limited assembly, Nat. Mater. 13 (2014) 301–307.
[3] P. Soukiassian, Hydrogen-induced nanotunnel opening within semiconductor subsurface, Nat. Commun. 4 (2800) (2013) 1–10.
[4] F. Wang, A. Dong, W. E. Buhro, Solution–Liquid–Solid Synthesis, properties, and applications of one-dimensional colloidal semiconductor nanorods and nanowires, Chem. Rev., DOI: 10.1021/acs.chemrev.5b00701.
[5] H. Goesmann, C. Feldmann, Nanoparticulate functional materials, Angew. Chem. Int. Ed. 49 (2010) 1362–1395.
[6] J. Tian, Z. Zhao, A. Kumar, R.I. Boughton, H. Liu, Recent progress in design, synthesis, and applications of one-dimensional TiO_2 nanostructured surface heterostructures: a review, Chem. Soc. Rev. 43 (2014) 6920–6937.
[7] C. Walkey, et al., Catalytic properties and biomedical applications of cerium oxide nanoparticles, Environ. Sci.: Nano 2 (2015) 33–53.
[8] A.B. Djurisic, X. Chen, Y.H. Leung, A.M.C. Ng, ZnO nanostructures: growth, properties and applications, J. Mater. Chem. 22 (2012) 6526–6535.
[9] R. Saravanan, N. Karthikeyan, V.K. Gupta, P. Thangadurai, V. Narayanan, A. Stephen, ZnO/Ag nanocomposite: an efficient catalyst for degradation studies of textile effluents under visible light, Mater. Sci. Eng. C 33 (2013) 2235–2244.
[10] R. Saravanan, N. Karthikeyan, S. Govindan, V. Narayanan, A. Stephen, Photocatalytic degradation of organic dyes using ZnO/CeO_2 nanocomposite material under visible light, Adv. Mater. Res. 584 (2012) 381–385.
[11] R. Saravanan, H. Shankar, T. Prakash, V. Narayanan, A. Stephen, ZnO/CdO composite nanorods for photocatalytic degradation of methylene blue under visible light, Mater. Chem. Phys. 125 (2011) 277–280.
[12] R. Saravanan, V.K. Gupta, V. Narayanan, A. Stephen, Visible light degradation of textile effluent using novel catalyst ZnO/γ-Mn2O3, J. Taiwan Inst. Chem. Eng. 45 (2014) 1910–1917.
[13] R. Saravanan, et al., ZnO/Ag/CdO nanocomposite for visible light-induced photocatalytic degradation of industrial textile effluents, J. Colloid Interface Sci. 452 (2015) 126–133.
[14] M.M. Mekonnen, A.Y. Hoekstra, Global gray water footprint and water pollution levels related to anthropogenic nitrogen loads to fresh water, Environ. Sci. Technol. 49 (21) (2015) 12860–12868.
[15] W. Boenne, N. Desmet, S.V. Looya, P. Seuntjens, Use of online water quality monitoring for assessing the effects of WWTP overflows in rivers, Environ. Sci.: Processes Impacts 16 (2014) 1510–1518.
[16] V.K. Gupta, I. Ali, T.A. Saleh, A. Nayak, S. Agarwal, Chemical treatment technologies for waste-water recycling—an overview, RSC Adv. 2 (2012) 6380–6388.
[17] A. Fujishima, K. Honda, Electrochemical photolysis of water at a semiconductor electrode, Nature 238 (1972) 37–38.
[18] X. Li, J. Yu, M. Jaroniec, Hierarchical photocatalysts, Chem. Soc. Rev. 45 (2016) 2603–2636.
[19] H. Wang, et al., Semiconductor heterojunction photocatalysts: design, construction, and photocatalytic performances, Chem. Soc. Rev. 43 (2014) 5234–5244.
[20] Q. Yu, J. Li, H. Li, Q. Wang, S. Cheng, L. Li, Fabrication, structure, and photocatalytic activities of boron-doped ZnO nanorods hydrothermally grown on CVD diamond film, Chem. Phys. Lett. 539 (2012) 74–78.
[21] V. Eskizeybek, F. Sarı, H. Gulce, A. Gulce, A. Avcı, et al., Appl. Catal. B Environ. 119−120 (2012) 197–206.
[22] R. Saravanan, et al., Enhanced photocatalytic activity of ZnO/CuO nanocomposites for the degradation of textile dye on visible light illumination, Mater. Sci. Eng. C 33 (2013) 91–98.
[23] S. Bhadra, D. Khastgir, N.K. Singha, J.H. Lee, Progress in preparation, processing and applications of polyaniline, Prog. Polym. Sci. 34 (2009) 783–810.
[24] U. Bogdanovic, et al., Interfacial synthesis of gold–polyaniline nanocomposite and its electrocatalytic application, ACS Appl. Mater. Interfaces 7 (51) (2015) 28393–28403.
[25] S. Yang, X. Cui, J. Gong, Y. Deng, Synthesis of TiO_2–polyaniline core–shell nanofibers and their unique UV photoresponse based on different photoconductive mechanisms in oxygen and non-oxygen environments, Chem. Commun. 49 (2013) 4676–4678.
[26] Z. Zhao, et al., Nanoporous TiO_2/polyaniline composite films with enhanced photoelectrochemical properties, Mater. Lett. 130 (2014) 150–153.
[27] R. Saravanan, V.K. Gupta, V. Narayanan, A. Stephen, Comparative study on photocatalytic activity of ZnO prepared by different methods, J. Mol. Liq. 181 (2013) 133–141.
[28] R. Saravanan, S. Joicy, V.K. Gupta, V. Narayanan, A. Stephen, Visible light induced degradation of methylene blue using CeO_2/V_2O_5 and CeO_2/CuO catalysts, Mater. Sci. Eng. C 33 (2013) 4725–4731.
[29] R. Saravanan, V.K. Gupta, E. Mosquera, F. Gracia, V. Narayanan, A. Stephen, Excellent visible light photocatalytic activity of β-Ag0.333V2O5 nanorods by facile thermal decomposition method, J. Saudi Chem. Soc. 19 (2015) 521–527.
[30] R. Saravanan, E. Thirumal, V.K. Gupta, V. Narayanan, A. Stephen, The photocatalytic activity of ZnO prepared by simple thermal decomposition method at various temperatures, J. Mol. Liq. 177 (2013) 394–401.
[31] S.E.S. Saeed, M.M.E. Molla, M.L. Hassan, E. Bakir, M.M.S.A. Mottaleb, M.S.A.A. Mottaleb, Novel chitosan-ZnO based nanocomposites as luminescent tags for cellulosic materials, Carbohydr. Polym. 99 (2014) 817–824.
[32] T. Witnoon, T. Permsirivanich, M. Chareonpanich, Chitosan-assisted combustion synthesis of CuO–ZnO nanocomposites: effect of pH and chitosan concentration, Ceram. Int. 39 (2013) 3371–3375.
[33] G. Rajasudha, H. Shankar, P. Thangadurai, N. Boukos, V. Narayanan, A. Stephen, Preparation and characterization of polyindole–ZnO composite polymer electrolyte with $LiClO_4$, Ionics 16 (2010) 839–848.
[34] D. Jassby, J.F. Budarz, M. Wiesner, Impact of aggregate size and structure on the photocatalytic properties of TiO_2 and ZnO nanoparticles, Environ. Sci. Technol. 46 (13) (2012) 6934–6941.
[35] M. Radoicic, et al., Improvements to the photocatalytic efficiency of polyaniline modified TiO_2 nanoparticles, Appl. Catal. B Environ. 136−137 (2013) 133–139.